PROCEEDINGS OF THE INTERNATIONAL CONFERENCE ON THE IONOSPHERE

LONDON JULY 1962

THE INSTITUTE OF PHYSICS
AND THE PHYSICAL SOCIETY

PROCEEDINGS OF THE
INTERNATIONAL CONFERENCE
ON

The Ionosphere

HELD AT

IMPERIAL COLLEGE
LONDON
JULY 1962

Published by
THE INSTITUTE OF PHYSICS AND THE PHYSICAL SOCIETY
1 Lowther Gardens, Prince Consort Road, London, S.W.7
Distributed by
Chapman & Hall, Ltd., 37 Essex Street, London, W.C.2
1963

CONTENTS

IRREGULARITIES AND DRIFTS IN THE IONOSPHERE

THE MATHEMATICS OF WAVE PROPAGATION THROUGH THE IONOSPHERE

PRELIMINARY RESULTS FROM THE FIRST ANGLO-AMERICAN SATELLITE UK1, ARIEL

IONOSPHERIC CONSTITUTION AND IONIZING RADIATIONS

Ionospheric constitution and ionizing radiations

H. FRIEDMAN

U.S. Naval Research Laboratory, Washington 25, D.C., U.S.A.

Abstract. The broad features of the structure of the atmosphere and its variability are described. Above 100 km, diffusive separation creates a composition dominated successively by atomic oxygen (200–800 km), helium (800–3000 km), and finally hydrogen (>3000 km). Molecular ions, O_2^+ and NO^+, characterize the lower ionosphere, and are gradually replaced at higher altitudes by the atomic ions O^+, He^+ and H^+. NO^+ is still present high in the F region and N^+ never exceeds a few per cent of the ion composition. The rate of ionization by solar x-ray and ultra-violet emission can be quite clearly defined, but the complex electron loss processes that control the relative importance of different wavelength regions in contributing to the equilibrium electron density are still not adequately understood.

1. Introduction

Considerable data have accumulated in recent years on density at satellite altitudes, but our knowledge of atmospheric structure below 200 km is still inadequate. Neutral particle concentrations, except for molecular oxygen, have not been measured directly but ion composition data from mass spectrometer measurements are available up to 900 km. Rocket-borne radio propagation experiments and plasma probes have outlined the profile of electron density to the limits of the terrestrial atmosphere and solar radiation measurements have mapped the altitude dependence of the spectral distribution of ionizing radiation to about 225 km. Yet, though we have experimental information concerning ion production, ion composition and the equilibrium electron density, the basic processes controlling the ionosphere are not quantitatively understood. The following paragraphs briefly review recent observations related to atmospheric and ionospheric structure, the spectrum of ionizing radiations and some interpretation of their interactions. The resulting picture defines many of the gross features of ionospheric structure and its production but it is still lacking in important details.

2. The structure of the atmosphere

Any theory of the ionosphere must include a model atmosphere, but the derivation of a model for the 90–200 km region is greatly handicapped by a lack of experimental data. Up to the beginning of the satellite era, the assortment of rocket measurements of atmospheric pressure, density, and temperature suffered from a variety of experimental uncertainties, with the values deduced for these parameters sometimes varying by several hundred per cent according to the methods used. In recent years the major effort has gone into satellite experiments, and rocket exploration of the region below 200 km has been relatively neglected. At the same time we have come to realize that strong diurnal, seasonal, solar cycle and solar activity induced variations in atmospheric structure must take place between 100 and 200 km. Present theories of the ionosphere must therefore

be based on somewhat loosely constructed models such as the COSPAR International Reference Atmosphere (CIRA).

2.1. *Neutral particle composition*

At ground level, the principal constituents of the atmosphere are molecular nitrogen, 78%, and molecular oxygen, 21%. The concentrations relative to air of the rare gases and other minor constituents such as CO_2 and methane are as follows:

Argon	Neon	Helium	Krypton	Xenon	CO_2	CH_4
$9{\cdot}3\times10^{-3}$	$1{\cdot}81\times10^{-5}$	$5{\cdot}2\times10^{-6}$	$1{\cdot}1\times10^{-6}$	$8{\cdot}7\times10^{-8}$	3×10^{-4}	$1{\cdot}5\times10^{-6}$

The first major change in atmospheric composition is the dissociation of oxygen near 100 km. Up to that level the atmospheric composition is maintained essentially constant by turbulent mixing. Near 100 km, diffusion begins to play an important role and results in a relative increase of the lighter constituents, hydrogen, helium, neon and oxygen, with increasing altitude. The hydrogen presumably is formed near the mesopause by the dissociation of water vapour and methane. From 200 km to about 800 km the composition is dominated by atomic oxygen. Helium may be the most abundant element between 800 and 3000 km and hydrogen forms the outermost atmosphere.

Dissociation of oxygen takes place as a result of absorption of solar radiation in the 1300 to 1750 Å region known as the Schumann continuum. Although the sun radiates as a 6000 degree black body in the visible region, the opacity of the solar atmosphere increases rapidly in the ultra-violet, and the effective temperature drops to about 4700°K near 1300 Å at solar maximum. The flux available for dissociation of oxygen is only 38 erg cm^{-2} sec^{-1} rather than the twenty-five times greater intensity that would be expected at 6000 degrees. Whereas the higher temperature flux would dissociate oxygen relatively abruptly and completely below the E region, at 4700°K dissociation is incomplete and an appreciable amount of O_2 diffuses to the F region.

2.2. *Exospheric helium*

The high atmospheric density derived from the rate of change of period of the Echo satellite led Nicolet (1961) to emphasize the importance of helium as an atmospheric constituent in the lower exosphere. Helium enters the terrestrial atmosphere as a result of the radioactive decay of ^{238}U and ^{232}Th. According to analyses of the abundance of these radioisotopes in the basalt and granite of the earth's crust, the outflow of helium is about 10^6 atoms cm^{-2} sec^{-1}. Since the total helium content of the atmosphere is about 10^{20} cm^{-2}, only 10^6 years are needed to produce all the atmospheric helium. This fixes the rate of escape and was used over a decade ago to estimate an exospheric temperature of no less than 1500°K.

The drag data on Echo 1 at 1500 km could not be accounted for by atomic oxygen since it would require a temperature much greater than 2000°K. Neither could it be explained by hydrogen since it would require an order of magnitude more hydrogen than is given by optical measures of the resonance absorption of solar Lyman-α. Assuming that complete mixing maintains the atmospheric concentration of helium relative to molecular nitrogen at $6{\cdot}7\times10^{-6}$ until diffusion begins near 105 km, Nicolet calculated a neutral

helium concentration of $8{\cdot}6 \times 10^5$ at 750 km and 1250°K. This amount of helium is adequate to explain the observed drag. Accordingly, helium supersedes atomic oxygen as the most abundant atmospheric constituent near 800 km.

2.3. *The geocorona*

The recognition of the existence of a hydrogen geocorona came as a result of observations of the Lyman-α glow of the night sky (Kupperian, Byram, Chubb and Friedman 1959). The average flux of this glow, 3×10^{-3} erg cm^{-2} sec^{-1} sterad^{-1}, exceeds the integrated visible flux of starlight and is comparable with the entire visible airglow. Simple theory, based on direct scattering of solar Lyman-α, led to the result that about $1{\cdot}3 \times 10^{12}$ neutral hydrogen atoms cm^{-2} column above 120 km were needed to produce the observed glow. Subsequently, a high resolution profile of solar Lyman-α was photographed from an Aerobee rocket, revealing a deep self-reversal due to neutral hydrogen between the rocket and the sun (Purcell and Tousey 1960). Analysis of the absorption core led to the result that the geocorona contained about 3×10^{12} atoms cm^{-2} above 100 km at a temperature of about 1100°K. Finally, a measurement of the ratio of overhead night sky glow to back-scattered albedo was made from a rocket that reached 1000 km. The densities computed from these data were 2×10^4 cm^{-3} at 400 km and $1{\cdot}4 \times 10^4$ at 1000 km (Kreplin, Friedman, Chubb and Mange 1962).

No single theory satisfactorily accounts for the three sets of data mentioned above. Mange (1961) and Bates and Patterson (1961) have computed thermospheric models and Chamberlain (1960), Johnson and Fish (1960), and Opik and Singer (1959, 1961) have developed exospheric models. Brandt (1961) has proposed an enhanced distant extension of the hydrogen atmosphere, a geocoma. It leaves the possibility of a thermosphere containing 2×10^{12} hydrogen atoms cm^{-3} above 120 km, an exosphere containing $1{\cdot}3 \times 10^{12}$ cm^{-3} above 150 km, and the geocoma containing 1×10^{12} cm^{-3}, with the centre of mass of the distribution near 15 earth radii. The hydrogen at this distance and beyond is identified with the escape component of the exosphere.

2.4. *Temperature and density variations*

Normal diurnal density variations as great as a factor of 10 at 1000 km were discovered in the course of analysis of satellite drag data, notably by Jacchia (1960), Priester (1959), King-Hele and Walker (1961) and Paetzold and Zschörner (1961). Drag effects are concentrated near perigee and as the plane of the orbit rotates in space, the perigee point moves from night to day and back again. In this way the perigee data over a period of time map out the diurnal variation. It was also found that the density of the upper atmosphere responded instantly to fluctuations in solar electromagnetic radiation, and to the arrival of plasma clouds signalled by geomagnetic storms.

For the altitude range 350 to 750 km, Priester and Jacchia have demonstrated a very close correlation between solar decimetre wave emission and fluctuations in orbital periods. According to Jacchia, the night-time temperature between 1958 and 1961 was related to the solar microwave flux according to

$$T_{\text{midnight}} = (555 + 3s)\ ^\circ\text{K} \qquad (1)$$

where the s unit is 10^{-22} watt m^{-2} c^{-1} sec^{-1} at 10·7 cm. The solar flux decreased over the three-year interval from $s = 350$ to $s = 90$, and the night-time temperature from 1600°K

to 800°K. The ratio of noon to midnight temperatures was about 1·35 corresponding to a difference of 500 to 300 degrees K between day and night.

The temperature variations produced by magnetic storms can be expressed by

$$\Delta T = 1 \text{ deg K}(Ap) \tag{2}$$

where Ap is the daily geomagnetic planetary index. Records of the past few years show that the atmospheric density may vary by a factor of 100 and the temperature by several hundred degrees in response to extremes of solar activity. From the correlation with ten centimetre data it is possible to predict the thermospheric temperature several years ahead. For example the minimum night-time temperature should reach approximately 500°K in 1964, the next sunspot minimum.

According to Jacchia, when the daily thermospheric temperature is corrected to a standard solar flux, there remains a systematic temperature decrease that roughly parallels the smoothed values of 10 cm solar flux. This effect could be accounted for by assuming

$$\Delta T = 4{\cdot}5 \text{ deg K } (\Delta s) \tag{3}$$

but then the sporadic changes are over-corrected. He therefore concludes that the systematic temperature decrease from 1958 to 1961 is related to an eleven-year cyclic corpuscular effect. This implies a normal corpuscular heating comparable to heating by electromagnetic radiation. Before accepting this conclusion it should be recognized that the ionizing radiation and 10 cm flux may be strongly correlated, but not strictly proportional. For example, in comparing the brightness of x-ray sources and 10 cm sources on the sun for 19th April 1960, the brightness contrast of features of the 10 cm map did not exceed a factor of 10–20 whereas the corresponding x-ray features showed a contrast of at least 70. In addition, the solar cycle variation of x-ray flux from the quiet sun appears to be substantially greater than the variation in 10 cm flux.

3. Electron density measurements

Electron density measurements by means of rocket-borne electron and ion probes, impedance probes, the Faraday effect, and radio wave dispersion techniques provide a fairly consistent picture of the distribution of electron density against height. Examples of typical results obtained by some of the above methods are shown in figures 1 and 2. The results indicate that the ionosphere has one principal maximum at around 300 km and that there exists only a shallow minimum between E and F. Jackson and Bauer (1961) found that the log of electron density against altitude above the F_2 peak exhibited a practically constant slope representative of diffusive equilibrium in an isothermal ionosphere. The scale height of the electron ion gas was 200 km and the electron temperature, assuming the mean ionic mass = 16, was 1640 ± 90°K for altitudes between 350 and 600 km (27th April 1961, 1502 E.S.T., Wallops Island, Virginia).

Using the Langmuir probe technique, L. G. Smith (1961) measured electron densities in the E region at night. The measurements showed a main layer about 20 km thick centred near 102 km. Superposed on this broad layer were regions of considerably greater N_e but of vertical dimensions of the order of only 1 km. Some of these layers are apparently due to sporadic-E and have large horizontal extent whereas others are highly localized and presumably are diffused meteor trails.

The thickness of the main E layer was roughly equal to the noon dimension but the level was lower at night by about 8 km. For two flights, 17th August and 27th October 1961, the measured maximum electron densities were 3×10^3 and 1×10^3 cm^{-3}. Since the first flight occurred three hours after sunset and the second at eleven hours, the results suggest

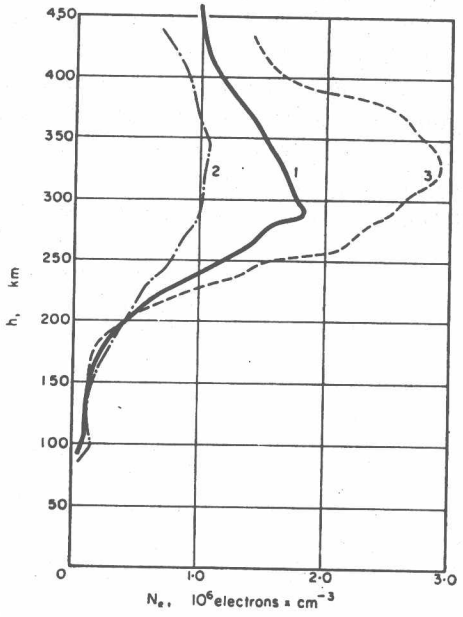

Figure 1. Electron density against altitude obtained by rocket-borne dispersion experiment. (1), 21st Feb 1958, 11: 40 ; (2), 27th Aug. 1958, 8 : 06; (3), 31st Oct. 1958, 15 : 54 (Gringauz and Rudakov 1961).

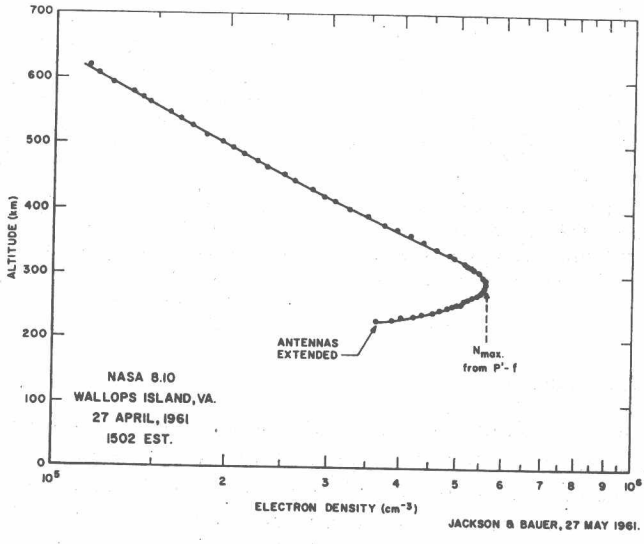

Figure 2. Ionospheric electron density distribution measured by means of Seddon's (1953) CW propagation technique from rocket that reached 620 km above Wallops Island, Va.

a decay of ionization with a recombination coefficient of $2{\cdot}3 \times 10^{-8}$ cm^3 sec^{-1} and an extrapolated maximum density at sunset of $1{\cdot}3 \times 10^4$ cm^{-3}. It was concluded that there was no evidence for any significant source of ionization in the night-time E region. In the trough above the maximum of E region, the flight shortly after sunset showed a reduction of the electron density to about 200 cm^{-3} in contrast to the relatively shallow trough observed in the day-time. It is clearly important to repeat a series of such experiments during the course of a single night.

Istomin (1961a) has reported mass spectrometer measurements at night of N_2^+, Mg^+, Ca^+ and Fe^+ in the E region. The concentration observed was about 10^4 cm^{-3} for Mg^+. Accordingly, he concluded that ionization by meteors is an important source of night-time E. Again, such experiments must be repeated to determine whether the results were typical of normal conditions or represented a diffused meteor trail.

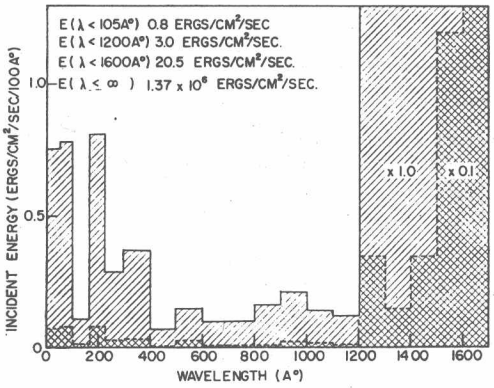

Figure 3. Spectral energy distribution of solar radiation from 0–1600 Å. After data of Detwiler, Garrett, Purcell and Tousey (1961), Kreplin (1961) and Watanabe and Hinteregger (1962).

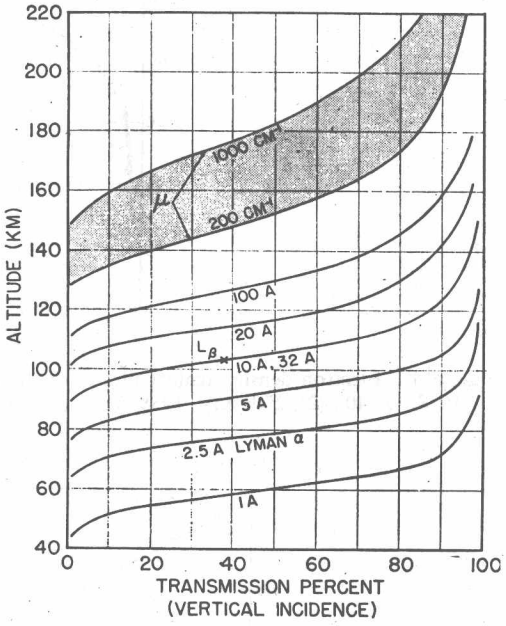

Figure 4. Penetration of the atmosphere by solar x-rays and ultra-violet radiation. The shaded portion includes the broad range of wavelengths from 100 to 850 Å for which the linear absorption coefficients lie between 200 and 1000 cm^{-1} (Friedman 1960).

4. Production of the ionosphere

The spectral energy distribution of far ultra-violet radiation and x-rays from the quiet sun is summarized in figure 3 for sunspot maximum. Figures 4 and 5 illustrate the theoretical transmission of the atmosphere for various wavelengths. Uncertainties in the atmospheric models and absorption cross sections, however, require that these curves be treated as only approximately correct. With these data it is possible to discuss the production of the ionosphere in a qualitative manner.

4.1. *The D region*

The problem of the D region has been analysed most recently by Nicolet and Aikin (1960). Under normal conditions the D region is taken to be the 60–90 km altitude span and the ionization is attributed to cosmic rays and Lyman-α. The maximum electron density is about 10^3 cm^{-3} and occurs near 80 km.

Cosmic ray primaries produce between 100 and 300 ion pairs per cubic centimetre per second between geomagnetic latitude 40 degrees and 60 degrees at sea level pressure. At any altitude where the particle density is n, the ionization rate, q, at latitude Φ is given by

$$q(\Phi) = q_0(\Phi)\,\frac{n}{n_0}\,. \tag{4}$$

Using $n_0 = 2{\cdot}5 \times 10^{19}$ cm^{-3},

$$q(\Phi = 50°) = 10^{-17}\, n \text{ cm}^{-3} \text{ sec}^{-1}. \tag{5}$$

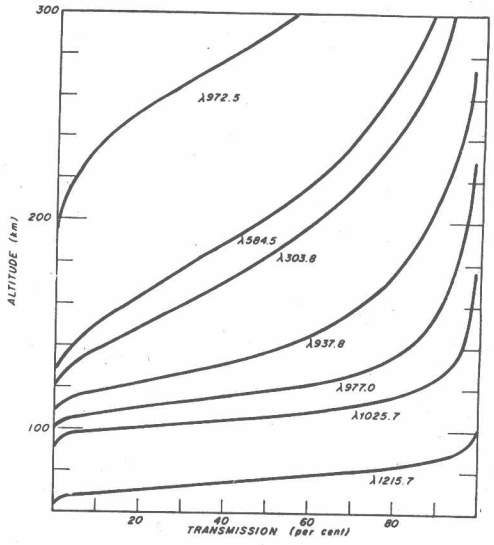

Figure 5. Penetration of the atmosphere by solar ultra-violet radiation (Watanabe and Hinteregger 1962).

For all electromagnetic radiation capable of ionizing molecular nitrogen or oxygen, the absorption cross section is greater than 10^{-18} cm^2, which places the level of unit optical depth above the D region (number of molecules per cm^2 column above 85 km $= 10^{20}$). To reach the D region, the wavelength must therefore be longer than 1026·5Å, the ionization potential of O_2 and must fit one of the windows in the O_2 absorption spectrum near 1108Å, 1143Å, 1157Å, 1167Å, 1187Å and 1216Å. The window at 1216Å matches Lyman-α perfectly, which makes it possible for the strong solar flux in the hydrogen resonance line to ionize the trace of nitric oxide that exists in the D region (E_i nitric oxide = 9·4 ev). Experimentally, Lyman-α is observed by means of rockets to penetrate to 75 km when the sun is overhead. Measurements made since 1957 yield fluxes between 6 and 3 erg cm^{-2} sec^{-1}. Although earlier measurements during the 1953 to 1955 sunspot period indicated

fluxes of a few tenths of an erg cm^{-2} sec^{-1}, there is now some doubt as to the validity of those solar minimum values (Friedman 1961).

Nicolet's estimate of the concentration of nitric oxide at 85 km is about 10^{-10} of the total concentration, or only 10^4 per cubic centimetre. This estimate is based on the production of nitric oxide by

$$N + O_2 \rightarrow NO + O \tag{6}$$

with atomic nitrogen being supplied through the ionization of molecular nitrogen by solar x-rays followed by dissociative recombination.

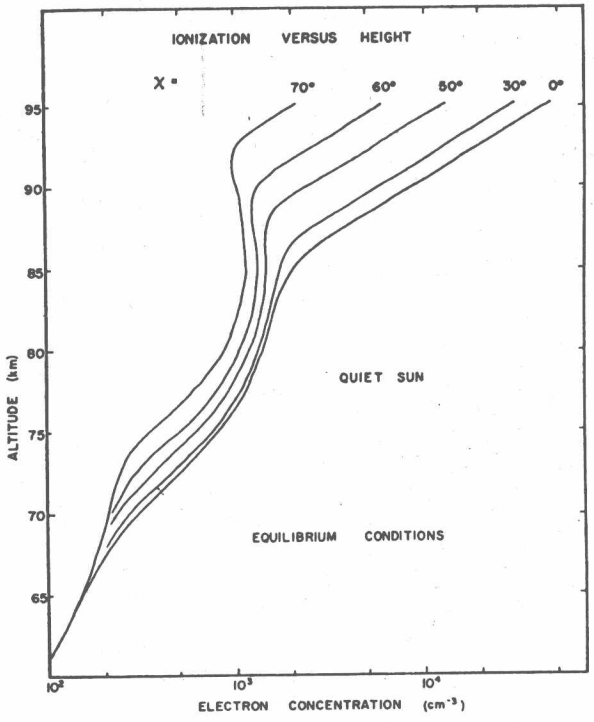

Figure 6. Electron density distribution in the D region as a function of solar zenith angle (Nicolet and Aikin 1960).

Adopting the following values for dissociative recombination coefficients,

$$\alpha_d(N_2) = 5 \times 10^{-7} \text{ cm}^3 \text{ sec}^{-1}, \tag{7}$$

$$\alpha_d(O_2) = 3 \times 10^{-8} \text{ cm}^3 \text{ sec}^{-1}, \tag{8}$$

$$\alpha_d(NO) = 3 \times 10^{-9} \text{ cm}^3 \text{ sec}^{-1}, \tag{9}$$

and including the effects of negative ion formation (negligible above 80 km, but important below 70 km), Nicolet and Aikin arrived at the D region electron density profile shown in figure 6. The effect of cosmic rays is apparent in the region below 70 km. Lyman-α produces the maximum in the distribution for an overhead sun near 85 km. At the mesopause, ionization is contributed by the tail of the x-ray spectrum.

4.2.1. *The E region.* The altitude range from 90–140 km may be referred to as the E region. Peak electron density is about 10^5 cm^{-3} at sunspot minimum and increases about 50 per cent at sunspot maximum.

For the production of the E region, the effective solar radiations are x-rays (10–100 Å), Lyman-β (1025·7 Å), C III (977 Å), and the Lyman continuum (910–800 Å).

The x-ray range may be divided into two parts, 10–31 Å and 31–100 Å, having comparable absorption cross sections. The division is produced by the K absorption edge of nitrogen. Although the shorter wavelength range, 10–31 Å, has been found to be highly variable over the solar cycle, it contains far less energy than the 31–100 Å range which accounts for most of the E region ionization. Over the past solar cycle the sun has been monitored in two bands, 8–18 Å and 44–60 Å (Kreplin 1961). Under quiet conditions the observed solar cycle variations have been factors of 45 and 7 respectively with the flux at maximum being about 0·7 erg cm^{-2} sec^{-1} for the entire 10–100 Å band. From the penetration curves of figure 4 it is apparent that x-ray ionization will spread over the entire range of the E region with a maximum effect near 120 km.

Lyman-β (figure 5) reaches unit optical depth at about 105 km; C III, 977 Å, at about 115 km; and the Lyman continuum at about 140 km. Since the nitrogen molecule exhibits band structure in its absorption of the Lyman continuum, there may be appreciable penetration within the bands to 120 km. Near solar maximum the observed flux at Lyman-β was about 0·05 erg cm^{-2} sec^{-1} and at C III (977 Å) about 0·08 erg cm^{-2} sec^{-1} (Watanabe and Hinteregger 1962). Both of these lines ionize molecular oxygen exclusively. Between 796 Å, the threshold for ionization of N_2, and 911 Å, the onset of ionization of atomic oxygen, the Lyman continuum contains about 0·36 erg cm^{-2} sec^{-1} (Detwiler, Garrett, Purcell and Tousey 1961). In this range, absorption by atomic oxygen sets in at relatively high altitudes and is the major source of attenuation, except for those wavelengths in the continuum that are absorbed by the band structure of N_2 in which the cross section reaches values as high as 10^{-16} cm^2 at certain wavelengths and as low as 10^{-18} cm^2 for others.

If one simply adds up the ultra-violet fluxes mentioned above, the total is 0·5 compared with 0·7 erg cm^{-2} sec^{-1} for x-rays at solar maximum. At solar minimum the x-ray flux was observed to decline to about 0·13 erg cm^{-2} sec^{-1} but no comparable data are available for the ultra-violet. Extrapolations based on the observed concentrations of Lyman-α in plage regions indicate that the ultra-violet emission associated with plages would be expected to show at least a 50 per cent decrease in intensity at solar minimum relative to solar maximum. Undoubtedly, quantitative data will become available within the 1963–1964 solar minimum period. Restricting our present considerations to solar maximum, it appears that the x-ray energy deposited in the E region exceeds the ultra-violet.

The step from rates of ionization to the determination of equilibrium electron density becomes quite complicated because the various ion species formed by photoelectric effect, N_2^+, O_2^+, O^+, recombine at different rates and may interact with the neutral atmosphere to form new ion species such as NO^+. Most laboratory measurements have indicated very rapid dissociative recombination for N_2^+ compared with O_2^+, as listed above in the reference to Nicolet and Aikin. If those values are applied to the E region, the x-ray ionization of N_2^+ can lead to no significant contribution to the equilibrium electron density. Four-fifths of the x-ray energy absorbed would have no influence on E region density and one would conclude that the ionization by ultra-violet is more important. (It is assumed that ionization is produced by x-rays with essentially equal efficiency in all constituents

at the rate of about 35 electron volts per ion pair and that the efficiency of photoelectric absorption of the ultra-violet radiations is about 50 per cent, or approximately 25 to 30 electron volts per ion pair.) One of the most recent laboratory investigations of the recombination rates for N_2 and O_2 (Kasner, Rogers and Biondi 1962, private communication) led to values of 6×10^{-7} cm^3 sec^{-1} and 4×10^{-7} cm^3 sec^{-1} respectively. If these recombination coefficients are correct, electron loss processes for N_2^+ and O_2^+ would proceed at more nearly the same rates and the relative importance of x-ray ionization would be enhanced.

The most significant clues to the importance of the various ionization processes come from mass spectrometer measurements of the relative ion composition. Mass spectrometer measurements (Johnson, Meadows and Holmes 1958, and Istomin 1961b) have shown that the dominant ion in the E region is NO^+ and that it persists in important concentration even into the F region (figure 7). At 110 km, according to Johnson *et al.*, the relative abundances of NO^+ and O_2^+ are 73% and 27% respectively. Bowhill (1961) estimated that to produce an equilibrium electron density of 10^5 per cubic centimetre NO^+ must be formed at the rate of 31 cm^{-3} sec^{-1} and O_2^+ at 270 cm^{-3} sec^{-1} if the dissociative recombination coefficients are 3×10^{-9} and 3×10^{-8} cm^{-3} sec^{-1} respectively.

O_2^+ can be produced both by x-rays and the ultra-violet lines, Lyman-β and C III. Since NO is only a trace constituent, formation of NO^+ by direct ionization cannot be of any significance. The most likely process leading to the large observed concentrations of NO^+ is

$$O^+ + N_2 \rightarrow NO^+ + N. \qquad (10)$$

Accordingly, the important step is the production of O^+. At 110 km the only effective source of O^+ is the x-ray spectrum. Assuming that four-fifths of the x-ray flux is 'wasted' on N_2 and that oxygen is 65% dissociated in the E region, about 13% of the total x-ray energy must be consumed in production of O^+. At solar maximum, then, we may expect about 0·1 erg cm^{-2} sec^{-1} of x-rays to produce the observed O^+ and thereby, according to (10), the NO^+. About 0·05 erg cm^{-2} sec^{-1} of x-rays and about 0·13 erg cm^{-2} sec^{-1} of Lyman-β and C III would produce O_2^+ directly. Only a relatively small portion of the Lyman continuum flux would be effective below 120 km. Since the production rate of NO^+ need be only one-ninth that of O_2^+ to account for the observed ion distribution, we may conclude that the x-ray flux is the controlling source of the E region between 100 and 130 km.

Referring again to the ion composition spectra of figure 7, careful examination of the telemetering records revealed no clear evidence of any N_2^+ ions. The sensitivity of the instrument was such that an N_2^+ concentration as great as 1% of the O_2^+ concentration would have been detectable. It is difficult therefore to understand the high value of $\alpha_d(O_2)$ found by Kasner *et al.* in laboratory experiments. If the recombination coefficient for N_2^+ and O_2^+ were so nearly alike, the amounts of these ions in the atmosphere should be almost comparable.

4.2.2. *E region eclipses.* Observations of the variation of solar x-ray and ultra-violet emissions during the Eclipse of 12th October 1958 in the South Pacific (Chubb, Friedman, Kreplin, Blake and Unzicker 1960) lend additional support to the theory of x-ray control of E region density. Several rockets were launched during the course of the eclipse including the totality phase, at which time 10 to 13% of the x-ray flux still remained whereas